

**INVESTIGATION OF INDUCTION HEATING OF
NON-FERROMAGNETIC METAL HALF-SPACE WITH
CORRUGATED SURFACE:
THE EXCITING MAGNETIC FIELD IS PARALLEL TO THE
ENVELOPING LINE OF THE CORRUGATED PROFILE**

László KOLLER, György TEVAN and István KISS

Department of High Voltage Engineering and Equipment
Budapest University of Technology and Economics
H-1521 Budapest Hungary

e-mails: koller@ntb.bme.hu, tevan@ntb.bme.hu, kiss@ntb.bme.hu

Received: April 25, 2002

Abstract

In this paper the electromagnetic field of a metal half-space with corrugated surface is investigated in the case when the exciting magnetic field is parallel to the enveloping line of the corrugated profile. The partial differential equation of the two-dimensional field computation is solved by the Galerkin method. A computer program has been developed to analyse the effects of different parameters.

Keywords: induction heating, Galerkin method, corrugated metal surface.

1. Introduction

The efficiency of induction heating is higher if the resistance of the heated load with invariance of the resistance of the inductor coil is higher. Decrease of the effective thickness of the eddy current increases the resistance of the charge and the efficiency. Therefore it is expedient to investigate the relations of quantities in the case of a metal load with a corrugated surface. The simplest case is a half-space metal with a sinusoidal corrugated surface, and the decrease of the effective thickness of the eddy current can be developed if the exciting magnetic field is parallel to the straight enveloping line of the corrugated profile. Based on the presented algorithm, a computer program was developed. It contains substitution of numerical values into the formulas and solution of a linear equation system, thus the detailed description of the program would unnecessarily increase the length of the paper.

2. The Mathematical Model

Fig. 1 shows the arrangement of the modelled infinitive half-space in a Descartes coordinate system, where the current exciter is supposed to be parallel to the surface

with infinitive length in y direction. The domain ‘air-gap’ can be another non-metal material as well. It follows from the model and from the arrangement of the excitation, that the field quantities are independent of the co-ordinate y , furthermore the electric field intensity has only y -component, and the magnetic field intensity has no y -component:

$$\frac{\partial}{\partial y} = 0, \quad \mathbf{E} = \mathbf{E}_y, \quad \mathbf{H}_y = \mathbf{0}. \quad (1)$$

Here and in the following the bold letters note (complex) phasors according to the sinusoidal time-dependent excitation with frequency ω . The Maxwell equations with respect to (1) are:

in load and also in air-gap:

$$\frac{\partial \mathbf{E}}{\partial x} = -j\omega\mu_0 \mathbf{H}_z, \quad (2)$$

$$\frac{\partial \mathbf{E}}{\partial z} = j\omega\mu_0 \mathbf{H}_x. \quad (3)$$

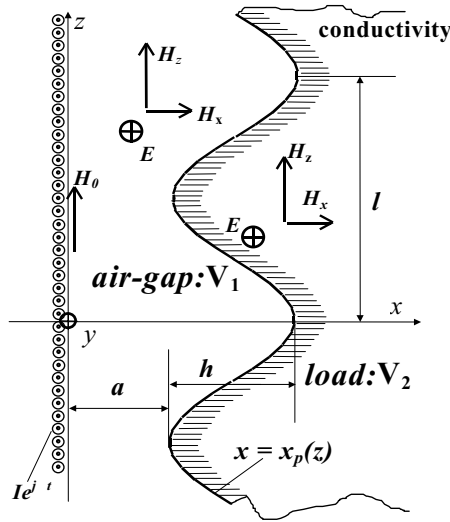


Fig. 1.

Because of unusually low frequencies and with a usual air-gap the displacement current can be neglected, therefore

in the load

$$\frac{\partial \mathbf{H}_x}{\partial z} - \frac{\partial \mathbf{H}_z}{\partial x} = \sigma \mathbf{E}, \quad (4)$$

in the air-gap

$$\frac{\partial \mathbf{H}_x}{\partial z} - \frac{\partial \mathbf{H}_z}{\partial x} = \mathbf{0},$$

where σ represents the conductivity of the load. Substituting (2) and (3) into (4) we can get

in the load

$$\frac{\partial^2 \mathbf{E}}{\partial z^2} + \frac{\partial^2 \mathbf{E}}{\partial x^2} = j\omega\mu_0\sigma \mathbf{E} \equiv \frac{2j}{\delta^2} \mathbf{E},$$

in the air-gap

$$\frac{\partial^2 \mathbf{E}}{\partial z^2} + \frac{\partial^2 \mathbf{E}}{\partial x^2} = \mathbf{0}, \quad (5)$$

where

$$\delta = \sqrt{\frac{2}{\sigma\omega\mu_0}} \quad (6)$$

is the skin depth. The z -component of the magnetic field intensity beside the exciting conductors is $(\mathbf{H}_z)_{x=0} = H_0 = \frac{NI}{l}$, where N turns are along length l of the periodicity. (I is real, the complex rms. value of the current). The boundary conditions for the electric field intensity are:

$$\left(\frac{\partial \mathbf{E}}{\partial x}\right)_{x=0} = -j\omega\mu_0 H_0 \quad \text{and} \quad \lim_{x \rightarrow \infty} \mathbf{E} = \mathbf{0}, \quad (7)$$

with respect to (2) and the infinity half-space of the metal conductors. In addition \mathbf{E} must be periodic in direction z , with periodicity l .

3. The Solution

Here the differential equation (5) with boundary conditions (7) will be solved with the *Galerkin* method. In the whole domain the following basis functions are selected so that they satisfy the prescribed boundary conditions:

$$\varphi_m(x, z) = \frac{\cos\left(2n \arctg \frac{x}{b}\right)}{\sqrt{1 + \left(\frac{x}{b}\right)^2}} \cos\left(\frac{2\pi k}{l} z\right); \quad (8)$$

$$m = kN + n + 1, \quad \begin{cases} k = 0, 1, 2, \dots, K - 1, \\ n = 0, 1, 2, \dots, N - 1, \\ m = 1, 2, 3, \dots, KN. \end{cases}$$

The basis functions are periodical in z direction with periodicity l , and satisfy the *homogeneous* boundary conditions (at $x = 0 \frac{\partial \varphi_m}{\partial x} = 0$ and at $x \rightarrow \infty \varphi_m = 0$), and form a complete set (MICHLIN, 1966). Here b is a suitable constant of length dimension in x . Thus, the electric field intensity can be expressed as:

$$\mathbf{E} \cong \sum_{i=1}^{KN} \mathbf{C}_i \varphi_i - j\omega\mu_0 H_0 f(x),$$

where

$$f(x) = \frac{x}{1 + \left(\frac{x}{b}\right)^2}, \quad (9)$$

$$i = \kappa N + \nu + 1, \quad \kappa = 0, 1, 2, \dots, K - 1, \\ \nu = 0, 1, 2, \dots, N - 1, \quad i = 1, 2, 3, \dots, KN.$$

The function $f(x)$ provides the inhomogeneous boundary condition at $x = 0$. The task is to determine the complex coefficient \mathbf{C}_i .

According to the *Galerkin* method, the inner product of all the basis functions φ_m with the differential equations (5) reduced to zero along the whole domain in the co-ordinate plane $x - z$ is:

$$\int_{(V_1)} \varphi_m \cdot \operatorname{div} \operatorname{grad} \mathbf{E} \, dV + \int_{(V_2)} \varphi_m \cdot \left(\operatorname{div} \operatorname{grad} \mathbf{E} - \frac{2j}{\delta^2} \mathbf{E} \right) \, dV = \mathbf{0}, \\ m = 1, 2, 3, \dots, KN,$$

where V_1 is the air-gap, and V_2 is the metal. With identities

$$\varphi_m \cdot \operatorname{div} \operatorname{grad} \mathbf{E} = \operatorname{div} (\varphi_m \operatorname{grad} \mathbf{E}) - \operatorname{grad} \varphi_m \cdot \operatorname{grad} \mathbf{E} \quad \text{and} \quad \mathbf{n} \cdot \operatorname{grad} \mathbf{E} = \frac{\partial \mathbf{E}}{\partial n}$$

and with the *Gaussian* formula we can obtain:

$$\int_{(V_1+V_2)} \operatorname{grad} \varphi_m \cdot \operatorname{grad} \mathbf{E} \, dV + \frac{2j}{\delta^2} \int_{(V_2)} \varphi_m \cdot \mathbf{E} \, dV - \int_{(\Gamma)} \varphi_m \frac{\partial \mathbf{E}}{\partial n} \, dA = \mathbf{0}, \\ m = 1, 2, 3, \dots, KN, \quad (10)$$

where Γ is a closed surface around the whole investigated region, and \mathbf{n} is the external normal vector of this surface. (It is sufficient to take length l of the region in z direction, because of the periodicity.) Due to the periodicity and the second equation of (7) it is easy to understand that only the integral along the plane $x = 0$ remains from the surface integral. On this plane the normal vector tends into $-x$,

therefore $\frac{\partial \mathbf{E}}{\partial n} = -\frac{\partial \mathbf{E}}{\partial x} = j\omega\mu_0 H_0$. So the expression (10) takes the following form:

$$\int_{(V_1+V_2)} \text{grad } \varphi_m \cdot \text{grad } \mathbf{E} \, dV + \frac{2j}{\delta^2} \int_{(V_2)} \varphi_m \cdot \mathbf{E} \, dV = j\omega\mu_0 H_0 \int_{(\Gamma_0)} \varphi_m \, dA, \quad (11)$$

$m = 1, 2, 3, \dots, KN$, and Γ_0 denotes the plane $x = 0$.

On the basis of (9) we can write

$$\begin{aligned} \text{grad } \varphi_m \cdot \text{grad } \mathbf{E} &= \frac{\partial \varphi_m}{\partial x} \frac{\partial \mathbf{E}}{\partial x} + \frac{\partial \varphi_m}{\partial z} \frac{\partial \mathbf{E}}{\partial z} \\ &= \sum_i \mathbf{C}_i \left(\frac{\partial \varphi_i}{\partial x} \frac{\partial \varphi_m}{\partial x} + \frac{\partial \varphi_i}{\partial z} \frac{\partial \varphi_m}{\partial z} \right) - j\omega\mu_0 H_0 f'(x) \frac{\partial \varphi_m}{\partial x}, \end{aligned}$$

furthermore,

$$\varphi_m \mathbf{E} = \sum_i \mathbf{C}_i \varphi_i \varphi_m - j\omega\mu_0 H_0 f(x) \varphi_m. \quad (12)$$

Taking unit length in y -direction and introducing the following matrix symbols:

$$P_{mi} = \int_{z=0}^l \int_{x=0}^{\infty} \left(\frac{\partial \varphi_m}{\partial x} \frac{\partial \varphi_i}{\partial x} + \frac{\partial \varphi_m}{\partial z} \frac{\partial \varphi_i}{\partial z} \right) dx \, dz, \quad (13)$$

$$Q_{mi} = \frac{2}{\delta^2} \int_{z=0}^l \left(\int_{x=x_p(z)}^{\infty} \varphi_m \varphi_i \, dx \right) dz,$$

where the equation of the corrugated surface:

$$x_p(z) = a + \frac{h}{2} \left[1 + \cos \left(\frac{2\pi}{l} z \right) \right] \equiv b\gamma(z), \quad (14)$$

$$q_m = \frac{1}{l} \int_{z=0}^l \int_{x=0}^{\infty} f'(x) \frac{\partial \varphi_m}{\partial x} \, dx \, dz, \quad (15)$$

$$w_m = \frac{2}{\delta^2 l} \int_{z=0}^l \left(\int_{x=x_p(z)}^{\infty} \varphi_m f(x) \, dx \right) dz, \quad (16)$$

$$s_m = \frac{1}{l} \int_{z=0}^l \varphi_m(0, z) \, dz. \quad (17)$$

Substituting (12)–(17) into (11) we obtain the following complex linear system of equations suitable to determine the complex coefficient \mathbf{C}_i .

$$\begin{aligned} \sum_{i=1}^{KN} P_{mi} \mathbf{C}_i + j \sum_{i=1}^{KN} Q_{mi} \mathbf{C}_i &= \omega\mu_0 H_0 l [-w_m + j(s_m + q_m)], \\ m &= 1, 2, \dots, KN. \end{aligned} \quad (18)$$

In knowledge of the coefficient \mathbf{C}_i the electric field intensity can be calculated from (8) and (9). Expressions for the magnetic field intensity can be obtained through (2), (3), (8) and (9):

$$\begin{aligned}\mathbf{H}_z &= \frac{j}{\omega\mu_0} \frac{\partial \mathbf{E}}{\partial x} = \frac{j}{\omega\mu_0} \left[\sum_{i=1}^{KN} \mathbf{C}_i \frac{\partial \varphi_i}{\partial x} + H_0 f'(x) \right], \\ \mathbf{H}_x &= -\frac{j}{\omega\mu_0} \sum_{i=1}^{KN} \mathbf{C}_i \frac{\partial \varphi_i}{\partial z}.\end{aligned}\quad (19)$$

To determine the active and passive power per unit surface propagating from the excitation toward the metal, the *average complex Poynting vector* must be averaged on length l of the corrugated surface because of the periodicity. The z -component of the magnetic field intensity and – with (8) and (9) – the electric field intensity at the inductor at $x = 0$ are

$$(\mathbf{H}_z)_{x=0} = H_0 = \frac{NI}{l}, \quad \mathbf{E}_0 = (\mathbf{E})_{x=0} = \sum_{m=1}^{KN} \mathbf{C}_m \cos\left(\frac{2\pi k}{l}\right).$$

Evaluating the required average of $H_0 \mathbf{E}_0$ only the terms with $k = 0$ remain, so the active and passive power per unit surface at the inductor can be expressed as:

$$\mathbf{S} = H_0 \sum_{m=1}^N \mathbf{C}_m = H_0 \sum_{m=1}^N \operatorname{Re}(\mathbf{C}_m) + j H_0 \sum_{m=1}^N \operatorname{Im}(\mathbf{C}_m) = P + jQ. \quad (20)$$

(The absolute values of field quantities are *rms* values, because current I is also an *rms* one.) To calculate the complex specific power transmitted into the conductive half-space through a plane boundary surface fitted to the top of the corrugated surface (and containing air, see Fig. 2)

$$S_w = P_w + jQ_w, \quad (21)$$

then the effective power component remains unchanged in (20) ($P_w = P$), but to determine Q_w , it is necessary to subtract the reactive power of the smallest air gap Q_a from Q . Thus, neglecting the distortion of the field caused by the corrugated surface, the reactive component of the transmitted power can be applied as:

$$Q_w = Q - Q_a. \quad (22)$$

Denoting field quantities by index 1 at $x = a$, we come to $Q_a = E_0 H_0 - E_1 H_1$. To obtain clearly arranged formulas, the distortion of H is not taken into consideration and $H_1 \cong H_0$, so $Q_a = E_0 H_0 - E_1 H_0 = (E_0 - E_1) H_0$. Finally, according to the induction law:

$$Q_a = H_0^2 \omega \mu_0 a = H_0^2 \frac{1}{\sigma \delta} \cdot \frac{2a}{\delta}. \quad (23)$$

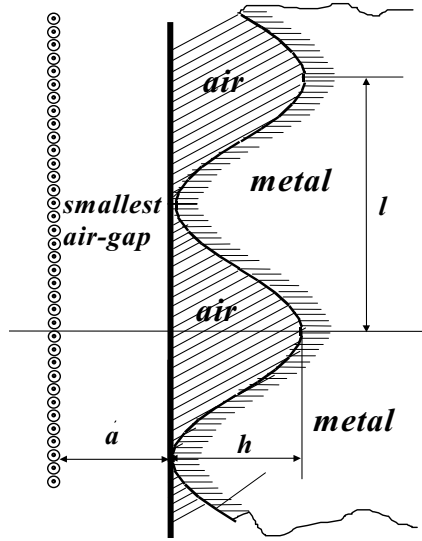


Fig. 2.

The influence of waviness

$$w = \frac{h}{l} \quad (24)$$

on the effective and reactive power can be examined by determining the complex power (S_P) per a unit surface in the case of a plane (zero waviness, $w = 0$) metal surface. According to the known relations:

$$S_P = H_0^2 \frac{1}{\sigma \delta} (1 + j) = P_P + j Q_P. \quad (25)$$

Introducing factors

$$\kappa_P = \frac{P_w}{P_p} \quad (26)$$

and

$$\kappa_Q = \frac{Q_w}{Q_p}, \quad (27)$$

they represent the ratio between the effective and reactive power per a unit surface of the infinite metal half-space having a corrugated surface closed by a plane and the power values of the infinite half-space with a plane surface. Otherwise, these numbers also give the ratio between the components of the complex inner impedance values (AC effective resistances and inner reactance values).

On the basis of the calculated results, it can be seen that κ_P and κ_Q are larger than 1. From the point of view of induction heating, the first result ($\kappa_P > 1$) is

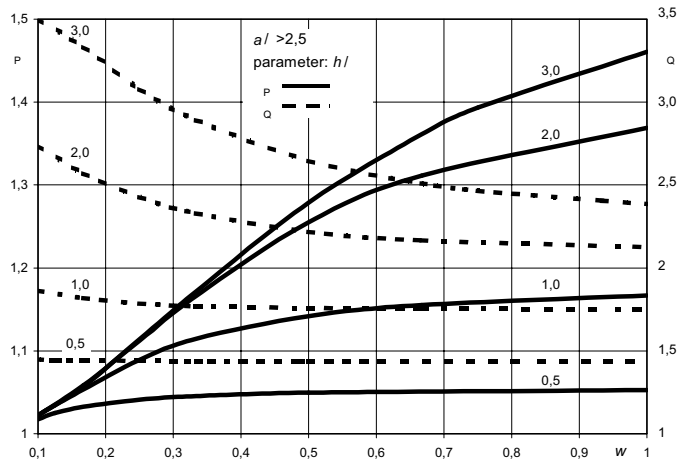


Fig. 3.

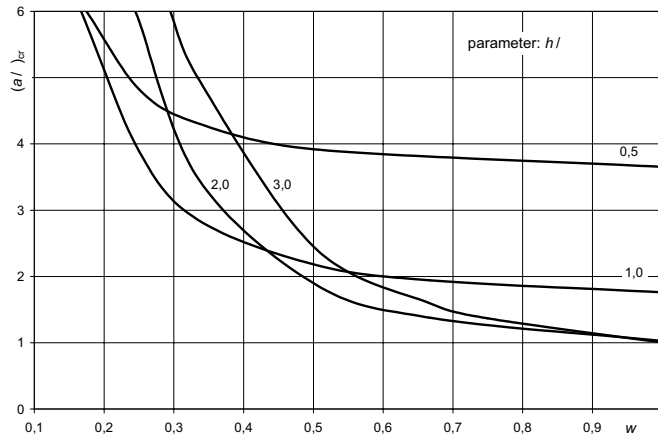


Fig. 4.

advantageous, because it means increasing electrical efficiency of the inductor load system. The last result ($\kappa_Q > 1$) seems to be disadvantageous, because it predicts a decreasing power factor ($\cos \varphi$) of the inductor load system. But it must be taken into consideration that the effective power is also greater, furthermore, the generated larger reactive power has a smaller weight in the resultant reactive power because of the reactive power of the additional air gap. To calculate the power factor, it would be necessary to know the complex power generated in the inductor coil, or to know the value of the inner impedance. However, it would not be practical to involve an inductor coil with a complicated geometry in the investigation, because

of the simplicity of the computational model. Thus, the quantitative comparison of the power factors must be discarded. Therefore the examinations will be carried out by taking into consideration only the air gap in the following way. Based on (22), (23) and (25), the following resultant reactive power can be obtained for a corrugated metal surface by an air gap with a thickness of a

$$Q = Q_w + 2Q_p \cdot \frac{a}{\delta} \quad (28)$$

and

$$Q' = Q_p \left(1 + 2 \cdot \frac{a}{\delta} \right), \quad (29)$$

for a plane metal surface. Ratio Q/P directly describes the power factor, because if it is smaller, the power factor is greater and vice-versa. Its value for a corrugated surface is

$$\frac{Q}{P_w} = \frac{Q_w}{P_w} + 2 \frac{Q_p}{P_w} \frac{a}{\delta},$$

while in the case of a plane metal surface it is

$$\frac{Q'}{P_p} = \frac{Q_p}{P_p} \left(1 + \frac{2a}{\delta} \right).$$

According to equation $Q_p = P_p$ and (26), (27),

$$\frac{Q}{P_w} = \frac{\kappa_Q}{\kappa_P} + \frac{2}{\kappa_P} \cdot \frac{a}{\delta} \quad (30)$$

and

$$\frac{Q'}{P_p} = 1 + \frac{2a}{\delta}. \quad (31)$$

Both quantities are linear functions of a/δ . In the following it can be seen, that $\kappa_Q > \kappa_P$ and $\kappa_P > 1$. Therefore there must be a critical a/δ ratio where the values of the two quantities are the same:

$$\left(\frac{a}{\delta} \right)_{cr} = \frac{\kappa_Q - \kappa_P}{2 \cdot (\kappa_P - 1)}. \quad (32)$$

This critical ratio is important because, in the case of $\frac{a}{\delta} > \left(\frac{a}{\delta} \right)_{cr}$ relation $\frac{Q}{P_w} < \frac{Q'}{P_p}$ is valid, so a load with a corrugated surface produces a better power factor.

4. Computational Results, Evaluation

The change of comparative factors (κ_P, κ_Q and $\left(\frac{a}{\delta} \right)_{cr}$) computed according to the method introduced above is shown in figures. The results are plotted as a function

of the waviness of the metal surface ($w = h/l$) in domain $0.0 \leq w \leq 1.0$ at different relative wave depths ($h/\delta = 0.5, 1.0, 2.0, 3.0$). At these parameters the variation of κ_P and κ_Q with respect to the relative air gap (a/δ) is small. Deviations larger than the computational and plotting error limit can only be demonstrated in domain $0.0 \leq a/\delta \leq 2.5$; the largest deviance values related to the case $a/\delta = 0$ are $\Delta\kappa_P = 2.21\%$, $\Delta\kappa_Q = -0.32\%$. The second small deviance confirms that the approximation introduced in (22) was correct. Therefore the diagrams representing the change of κ_P and κ_Q can be related to relative air gap values $a/\delta > 2.5$.

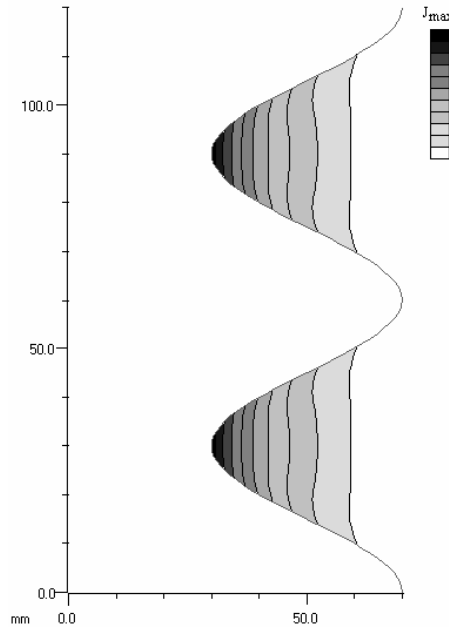


Fig. 5.

In Fig. 3 the change of κ_P and κ_Q can be seen. It can be noticed, that κ_P increases monotonously with increasing waviness (w) and relative wave-depth (h/δ), while κ_Q decreases monotonously with increasing w and decreasing h/δ .

The primary goal of the application of a load with a corrugated surface instead of a plane surface is to increase the efficiency of the inductor load system by increasing the effective power streaming into the load, namely, to obtain as high κ_P value, as possible. Even a large degree of power increment can be achieved. Its largest value in the investigated case is 46% ($\kappa_P = 1.46$) at $w = 1.0$ and $h/\delta = 3.0$. To obtain larger values than these parameters may hit against practical difficulties. Furthermore, it is not expedient to choose h/δ higher than 3.0, because – for example – at $h/\delta = 4.0$ only $\kappa_P = 1.4966$ can be achieved, which is only by 2.5% higher than the previous one. On the basis of Fig. 3, taking the change of κ_Q into consideration, it is practically recommended to choose the values of the parameters

in domains $0.4 \leq w \leq 1.0$ and $1.5 \leq h/\delta \leq 3.0$.

Fig. 4 represents the change of the values of the critical relative air gap $\left(\frac{a}{\delta}\right)_{cr}$. These values are strongly decreasing with increasing w up to approx. $w = 0.5$. Above that waviness, the grade of decrement is smaller. Curves connected to different h/δ parameters intersect each other. Anyway, it can be clearly seen that *choosing the parameters in domains $0.4 \leq w \leq 1.0$ and $1.5 \leq h/\delta \leq 3.0$ is useful not only from the point of the efficiency of the inductor load system, but from the aspect of the increment of the power factor as well.*

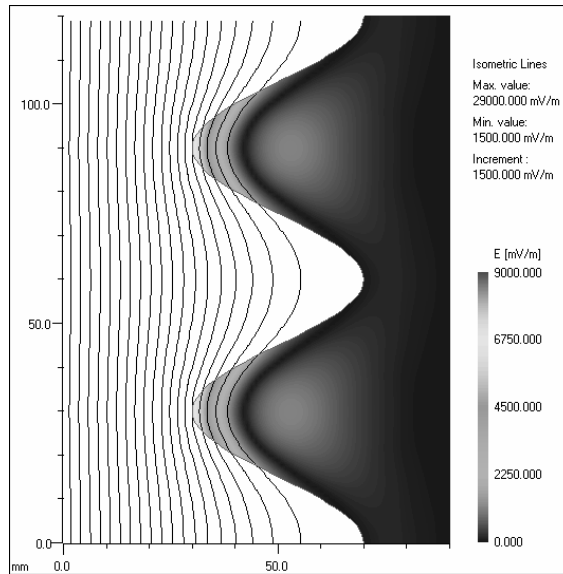


Fig. 6. Isometric lines of the absolute values of electric field strength, which are at the same time the field lines of the magnetic field in 2D, when the current of inductor is maximal.

Finally, in *Fig 5* the isometric lines of rms values of the electric field strength are plotted at $a/\delta = 3.0$, $w = 0.667$, $h/\delta = 4.0$. In the figure it can be seen that the electromagnetic waves practically cannot intrude into the bottom of the waves of the corrugated surface, therefore the current density is high at the top of the waves. Thus, the current density is not uniform in direction z – like it is in the case of a load with plane surface –, the available active cross-section is reducing, so the AC effective resistance of the load as well as the effective power generated in the load increase.

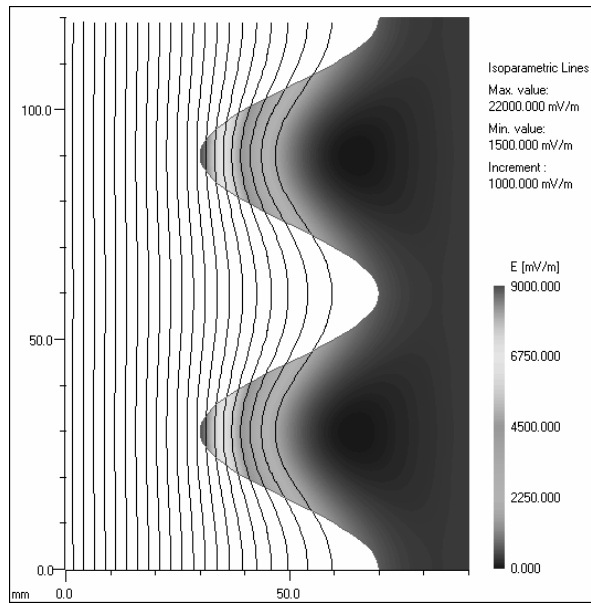


Fig. 7. Isometric lines of the absolute values of electric field strength, which are at the same time the field lines of the magnetic field in 2D, when the current of load is maximal.

Acknowledgements

The research was partially supported by the Hungarian National Research Foundation, project number: OTKA 025045.

References

- [1] SIMONYI, K., *Foundations of Electrical Engineering*, Oxford: Pergamon Press Ltd. 1963.
- [2] MIHLIN, S. G., *Variational Methods in Mathematical Physics*, New York: Macmillan, 1964.
- [3] MIHLIN, S. G., *Numerical Realization of Variational Method*, (in Russian), Izd. Nauka, Moscow, 1966.